Numerical Investigation of Natural Convection Loss in Cavity-Type Solar Receivers

S. PAITOONSURIKARN and K. LOVEGROVE
Centre of Sustainable Energy Systems,
Department of Engineering,
Australian National University,
Canberra ACT 0200,
AUSTRALIA
Telephone: +61 02 6125 8299
Facsimile: +61 02 6125 0506
E-mail: Sawat.Paitoonsurikarn@anu.edu.au

Abstract

In solar thermal systems, especially for high concentration applications, natural convection contributes a significant fraction of energy loss. Its characteristics hence need to be understood so that it can be effectively minimized in order to improve system efficiency. The present study numerically investigates the influence of cavity geometry and inclination on the convective loss through the aperture. The Computational Fluid Dynamics package "Fluent 6.0" has been used to investigate three cases of geometrically different receivers. The calculated heat loss results shows a nonlinear dependence on the inclination angle and shows qualitatively good agreement with those calculated by various previously proposed empirical models. The Clausing model (1981) shows the closest prediction to both numerical and experimental results despite its original use for larger-scale central receiver systems.

1 INTRODUCTION

The Australian National University (ANU) has been involved with the investigation of solar thermal energy conversion using paraboloidal dish concentrators for many years. Currently the team is undertaking R&D on a 400 m^2 concentrator fitted with a monotube boiler cavity receiver for superheated steam production and a 20 m^2 concentrator that operates a cavity receiver lined with reactor tubes for ammonia dissociation for energy storage (Johnston *et* al, 2001)&(Lovegrove *et* al, 2001)&(Luzzi *et* al, 2002). In such systems, the receivers experience three modes of heat loss; conduction loss through the wall, convection and radiation losses through the aperture all of which need to be minimized in order to improve the receiver performance. In general, conduction and radiation losses can be determined relatively easily using standard methods (e.g. Holman, 1997). On the other hand, the determination of convection loss is rather difficult and usually relies on semi-empirical models

This paper reports some initial results obtained from the simulation of the convection losses from the ANU dish receivers using the Computational Fluid Dynamics (CFD) package "Fluent". The study complements a parallel experimental investigation using an electrically heated model of a cavity receiver that is also reported in these proceedings (Taumoefolau 2002).

1.1 Previous Work

There have been several previous investigations of natural convection heat loss from open-cavities. Le Quere *et* al (1981) studied the heat loss from an isothermal cubic cavity in the range of $10^7 < Ra < 10^9$. The total heat loss was found to be strongly dependent on the cavity inclination and the correlation for each inclination was established. Clausing (1981) hypothesized that two factors governed the convective heat loss, i.e., (i) the ability to transfer mass and energy across the aperture and (ii) the ability to heat air inside the cavity. A simplified analytical method was developed based on the above assumption. He concluded that the latter factor was of greatest importance. Hess *et* al (1984) investigated the natural convection losses from horizontal rectangular cavities for large Rayleigh number ($Ra > 10^{10}$). They found that the use of a flow restriction at the aperture plane could reduce natural heat loss by about 10%. In addition to physical experiments, Eyler (1980) carried out the 2D simulation of the convective heat loss from large rectangular cavities whose dimensions (depth x height) were 2.59m x 2.88m and 12.95m x 14.35m. He found a non-linear dependence of heat loss with respect to cavity size, receiver inclination, and aperture diameter.

Notably, however, all of these investigations addressed large scale cavities such as those employed in central receiver applications and so the results need to be carefully verified if used for smaller scale ones. Among a handful of research

papers on small scale cavities applicable to solar dishes, Koenig and Marvin developed a heat loss model based on relatively high cavity temperature between 550°C and 900°C, which was summarized in the comprehensive review by Anderson *et a*l (1987). Stine *et* al (1989) extended the work by Siebers *et* al (1984), which was originally applicable only for central-receiver. They included the effects of varying aperture size and receiver inclination. Recently, Leibfried *et* al (1995) developed two new generalized models that can be used for both downward and upward facing cavities with various geometries. The two proposed models were based on another work by Clausing *et* al (1987) in which a model was derived from the experimental data from a cubical cavity, and by Stine *et* al (1989). The modifications of Clausing's and Stine's Models were primarily in order to take into account the different flow pattern while the cavity was facing upward and the effect of different geometries of the cavities. Leibfried verified the two modified models with experiments on spherical and hemi-spherical cavities and found very good agreement. The Rayleigh number in their experiment varied between 10^7 and 10^9, which implies that most of the flow regime was laminar.

Although there have been a few experimental models developed so far, their range of applicability for different cavity geometries is not clear.

2 NUMERICAL PROCEDURE

2.1 Problem Formulation

The CFD Software Package, Fluent 6.0 (Fluent Inc., 2002) is being employed in the 3D simulation of natural convection.

In reality, the receiver is surrounded by an infinite atmosphere with a limiting temperature equal to ambient air temperature. To model this condition in the CFD analysis, the flow domain is established such that the receiver is centrally placed in a sufficiently large enclosure with walls at ambient temperature as schematically shown in Fig. 1a. Figs. 2a to 2c illustrate the cross sections and relevant dimensions of the three receivers considered. The model shown in Fig. 2a represents the experimental receiver model constructed and characterized by Taumoefolau (2002). The other two shown in Figs. 2b and 2c are essentially the replications of the actual receivers currently employed in the ANU 20 m^2 and 400 m^2 dishes, respectively.

The size of the virtual enclosure was increased until it had an insignificant effect on the predicted fluid and heat flows in the vicinity of the receiver. Eyler (1980) stated that as long as the exterior region of the cavity extended beyond a distance about equal to the interior cavity depth, the effect on flow and heat transfer inside the receiver was negligible. However, in this study it was found that the diameter of the cylindrical enclosure should be about twenty times the diameter of the receiver to achieve this.

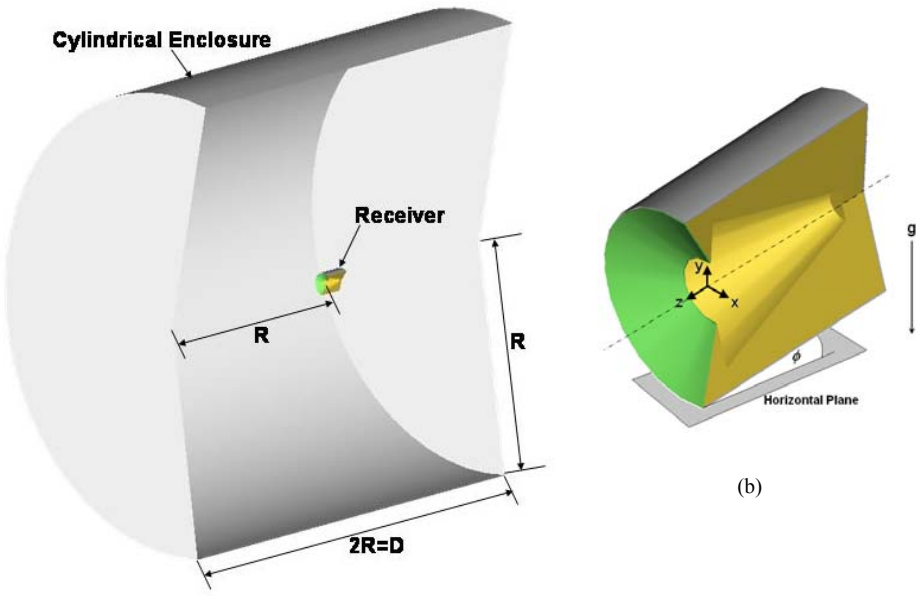

Fig. 1 Schematic diagram of flow configuration: (a) the receiver location in the entire domain, (b) the 20 m^2 dish cavity receiver showing the angle of inclination.

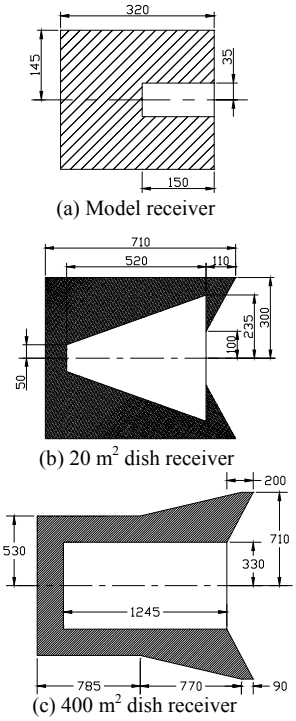

Fig. 2 Cross sectional diagram of all three receiver models.

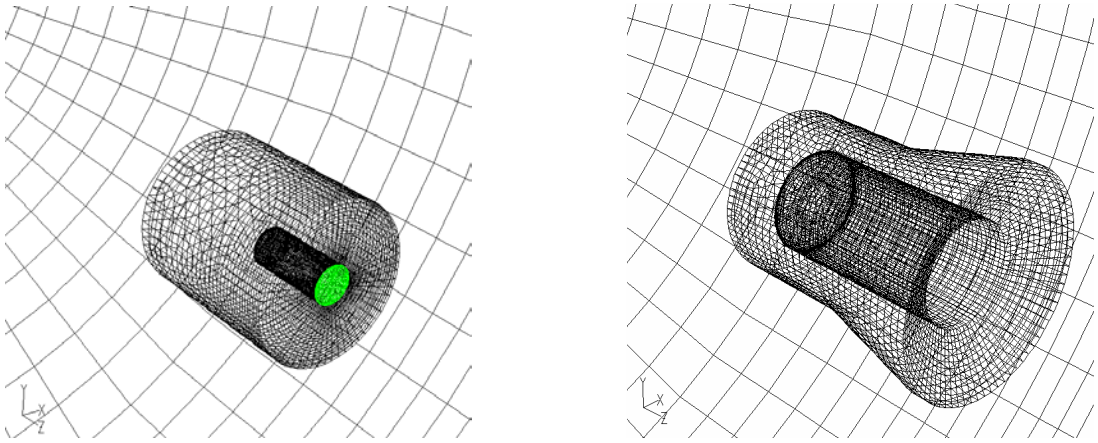

(a) (b)

Fig. 3 Typical computational grids for (a) model receiver and (b) 400 m^2 dish receiver.
Note that these figures also show the mirror image opposing across the symmetrical plane.

Grid dependency was investigated and the final grids used consist of approximately $2x10^5$ hexahedral cells. The cells are very small in the region inside the cavity and nearby the receiver but increase in size gradually toward the cylindrical enclosure wall. Fig. 3 shows the typical grids used for the laboratory model and 400 m^2 dish receiver cases.

2.2 Modeling Equations

The flow and heat transfer simulation is based on the simultaneous solution of the system of equations describing the conservation of mass, momentum, energy and turbulent transport property. The Spalart-Allmaras one-equation turbulent model recommended by Spalart (2000) is employed.
The steady-state governing equations are solved in Fluent using a coupled solver, which means that temperature and flow fields are coupled with each other and are solved simultaneously. All temperature-dependent properties of fluid, i.e. air, such as density are evaluated at local temperature by using the least-square fit equations derived from thermodynamic data compilations taken from (Holman, 1997).

2.3 Boundary Conditions

The isothermal boundary condition was applied to cavity wall, whereas the outer walls of the receivers were assumed to be adiabatic. The cavity wall temperatures used were:

- For the model receiver, the average experimental values of cavity wall temperature data of 445^{o}C and 408^{o}C were used for the cylindrical section and circular end plate, respectively.
- For the 20 m^2 dish receiver, the typical experimental data of cavity wall temperature data were used, which were 637^{o}C, 655^{o}C and 576^{o}C for the annular section surrounding the aperture, frustum section and circular back section, respectively.
- For the 400 m^2 dish receiver, the temperature of the whole cavity wall was arbitrarily set at 627^{o}C.

The wall temperature of the entire cylindrical enclosure was set to T_{amb}=27^{o}C. Normal velocity and normal gradients of all flow variables were set to zero across the vertical plane of symmetry. The inclination of the cavity as shown in Fig. 4b was simulated by redirecting the gravity vector to the desired direction. The gravitational constant was specified to the standard value of 9.80665 m/s^2.

2.4 Solution Criterion

The initial guesses for velocity, temperature, and turbulent viscosity fields were set to constant values over the entire computational domain. To obtain the flow and heat transfer solutions, the solver undertakes iteration until the convergence criterion is satisfied, which employs scaled residuals of the modified variables in the governing equations as the measure.
In addition, the averaged cavity wall heat flux was examined explicitly for convergence (to less than a 0.01% variation between iterations).
Typical computational time takes about 30 hours on one CPU of a Compaq ES45 Alpha 1-GHz machine.

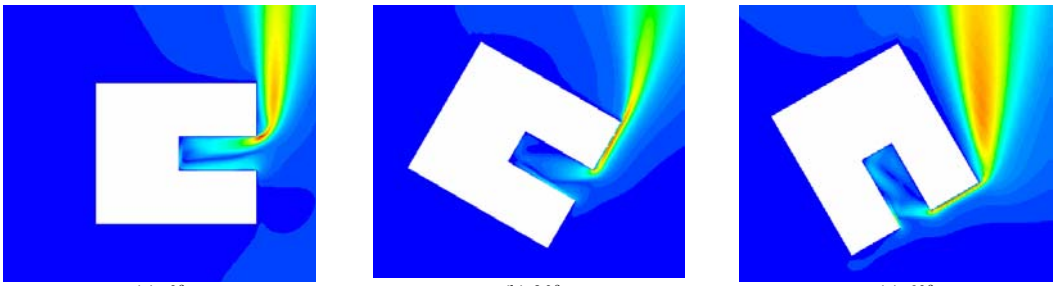

(a) 0° (b) 30° (c) 60°

Fig. 4 Contour plot of velocity magnitude at symmetry plane for model receiver.

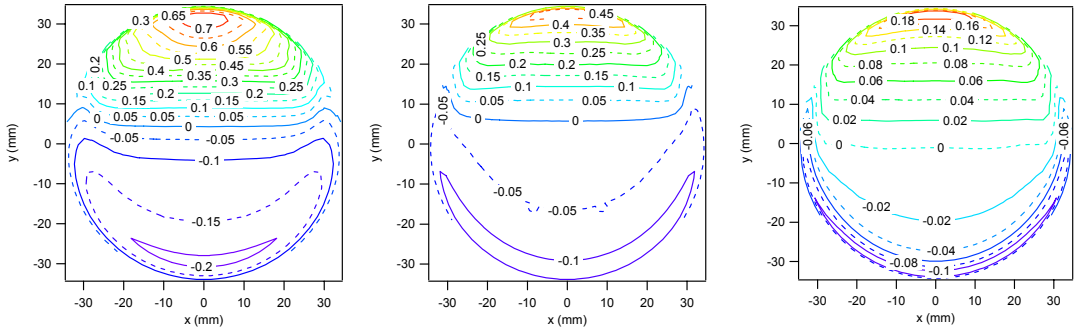

(a) 0° (b) 30° (c) 60°

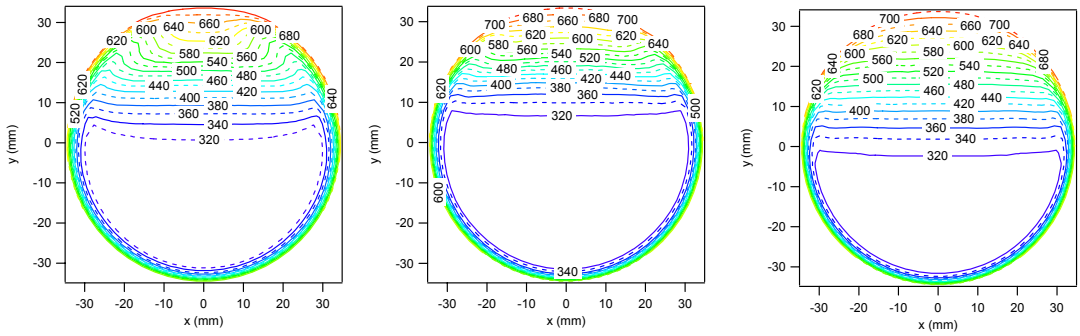

(d) 0° (e) 30° (f) 60°

Fig. 5 Profiles at aperture plane for model receiver: (a)-(c) normal velocity (m/s), (d)-(f) temperature (K).

3 RESULTS AND DISCUSSIONS

3.1 Results for Model Receiver

Contour plots of velocity magnitude in the symmetry plane of the model receiver at angles of 0°, 30°, and 60° are presented in Figs. 4a) to c). In each figure the color represents the relative magnitude and so cannot compare to those in other figures. It is evident that the predicted flow pattern is in agreement with what is intuitively expected. At an inclination angle of 0°, the cold air enters the cavity at the lower half of the aperture and flows along the lower part of the cavity where it is heated. The air reaches the back wall and flows upward until it encounters the upper cavity wall. The air then flows back along it and finally exits the cavity. A relatively stagnant core is observed in the middle of the cavity. The hot plume of air coming out from the upper half of the aperture flows directly upward without attachment to the frontal part of the receiver. The plume spreads out with decreasing velocity due to both the viscous effect and reduction of induced buoyancy force caused by cooling of the plume. The flow patterns at angles of 30° and 60° are quite similar but with the addition of a stagnant zone and local circulation in the upper part of the tilted cavity due to the stable stratification of temperature. In these cases the exiting hot plume attaches to the front of the receiver before separating at the receiver's edge and spreading out.

Figs. 5a) to f) show the corresponding profiles of normal velocity and temperature in the aperture plane. They clearly show that the inflow and outflow of air occupies the lower and upper halves of the aperture respectively. The maximum outflow velocity occurs near the top, whereas the maximum inflow velocity occurs near the bottom. The magnitude of both decreases with increasing angle. The inflow area is not significantly different between angles of 0° and 30°, just slightly greater for the latter, as can be seen from the area below the line of zero velocity depicted in Figs. 5a) and b).

However, for angle=60^o shown in Fig. 5c), the inflow area is reduced as a result of the flow blockage which is primarily caused by the augmentation of the stagnation region inside the cavity. The temperature of the bulk air entering the cavity is about 320 K (or 47^{o}C) in all cases, which is higher than the ambient temperature of 300 K. This shows that the incoming air is heated by mixing with the exiting hot plume before it enters.
The heat loss from the cavity was determined both from integrating the heat loss from the cavity wall and from the net enthalpy flow rate through the aperture. The agreement was within numerical accuracy.
The comparison between the present numerical and corresponding experimental results of convection loss together with those predicted from various previously proposed correlations is reported in the parallel paper by Taumoefolau (2002). It illustrates that all heat loss results decrease monotonically with increasing angle as also suggested by the flow fields shown in Fig. 4 and 5. The numerical results coincide with the experiment at the angle of inclinations = 0^o and 90^o, but shows the slight overestimation at intermediate angles. However, considering the uncertainty associated in both results, the agreement is considerably good.

3.2 Examination of ANU Receiver Geometries

CFD calculations have been applied to the geometries of the two cavity receivers on the ANU dishes. The results of flow and heat transfer characteristics for both are qualitatively similar to those of the model receiver shown in Figs. 4 and 5, despite the fact that the length scale and operating condition are different.
The calculated total heat losses are plotted in Figs. 6 and 7, together with the predictions of the various correlations identified in section 2. The CFD result lies in the same range of most of those predicted. The Stine and McDonald model shows the greatest deviation from the others. As stated in the work by Leibfried et al (1995), it tends to overestimate the convective losses at high cavity temperature and can be improved if the reference temperature is changed to film temperature, i.e., the average of cavity and ambient temperatures. This is one of the improvements employed in the modified Stine & McDonald model. The Koenig & Marvin model shows fairly good agreement with the numerical results, which correlates with the fact that it was derived from the data of actual receivers of similar sizes to those used on the ANU dishes. The Clausing model shows excellent agreement to the numerical results for the 400 m^2 dish receiver, whereas the modified Clausing and Stine & McDonald models do for the 20 m^2 dish receiver. Considering the uncertainty quoted in each correlation, the comparison shows that, despite their actual range of applicability, all correlations except the original Stine & McDonald model can predict the convective heat loss of the actual size receivers within a similar range and hence might be used interchangeably. Nonetheless, the original Clausing model is recommended as it can best correlate the present result in all cases considered including those from the experiment by Taumoefolau (2002).
Note that, all of the correlations examined predict zero natural convective loss at 90^o angle. This is physically implausible and indeed both the experimental measurements and CFD calculation from this study indicate that this is not the case.

4 CONCLUDING REMARKS

The numerical investigation of natural convection heat loss from cavity receivers of solar dishes has been carried out. The numerical results obtained are qualitatively in good agreement with those predicted by various previously proposed correlations. The Clausing model (1981) shows the closest prediction despite its original use for bigger-scale central

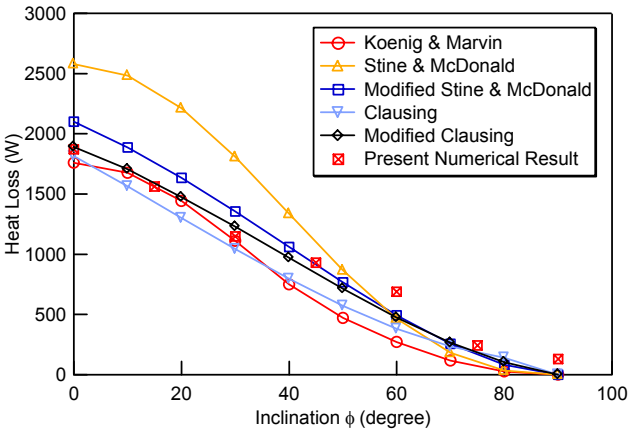

Fig. 6 Comparison of natural convection heat loss through the aperture for 20 m^2 dish receiver.

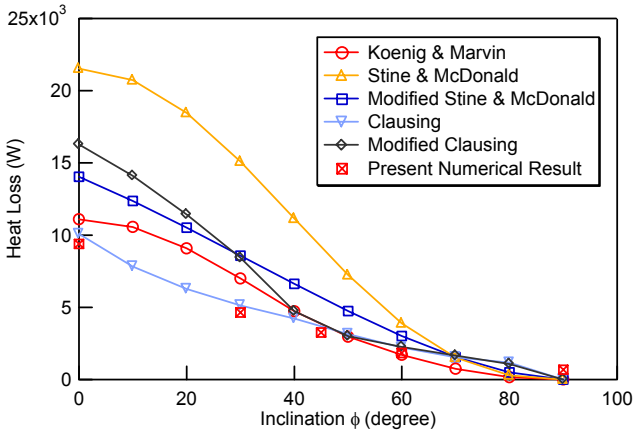

Fig. 7 Comparison of natural convection heat loss through the aperture for 400 m^2 dish receiver.

receivers. The discrepancy of convective heat loss at an orientation of 90^o between the present results and the predictions of correlations taken from the literature requires further investigation. More generalized study of mixed convection, i.e. including wind effect, will be conducted in the next step. The final goal is to develop an improved correlation that can reliably predict convective losses from cavity receivers on dish concentrators at all angles.

5 REFERENCES

Anderson R. and Kreith F. (1987), *Natural Convection in Active and Passive Solar Thermal Systems*, Adv. Heat Transfer 18, 1-86.

Clausing A.M. (1981), *An Analysis of Convective Losses From Cavity Solar Central Receiver*, Sol. Energy 27, 295-300.

Clausing A.M., Waldvogel J.M., and Lister L.D. (1987), *Natural Convection from Isothermal Cubical Cavities with A Variety of Side-Facing Apertures*, ASME J. Heat Transfer 109, 407-412.

Eyler L.L. (1980), *Prediction of Convective Losses from A Solar Cavity Receiver*, In Proceedings for the Century 2 Solar Energy Conference, San Francisco, California.

Fluent Inc. (2002), *Fluent 6 User Guide*.

Hess C.F. and Henze R.H. (1984), *Experimental Investigation of Natural Convection Losses from Open Cavities*, J. Heat Transfer 106, 333-338.

Holman, J.P. (1997), *Heat transfer*. 8th edition, New York: McGraw-Hill Companies.

Johnston G., Burgess G., Lovegrove K., and Luzzi A. (2001), *Economic Mass Producible Mirror Panels for Solar Concentrators*, Proceedings of ISES World Congress, Adelaide, Australia.

Leibfried U. and Ortjohann J. (1995), *Convective Heat Loss from Upward and Downward-Facing Cavity Solar Receivers: Measurements and Calculations*, J. Sol. Eng. 117, 75-84.

LeQuere P., Penot F., and Mirenayat M. (1981), *Experimental Study of Heat Loss through Natural Convection from An Isothermal Cubic Open Cavity,* Proceedings DOE/SERI/SNLL workshop on convective losses from solar receivers, Sandia Laboratory Report SAND81-8014, Livermore, California, 165-174.

Lovegrove K., Luzzi A., Soldiani I., and Kreetz H. (2001), *Developing Ammonia Based Thermochemical Energy Storage for Dish Power Plants – Smelly Experiments, Good Technology*, Proceedings of ISES World Congress, Adelaide, Australia.

Luzzi A., Lovegrove K., Paitoonsurikarn S., Siangsukone P., Johnston G., Burgess G., Joe W., and Major G. (2002), *Paraboloidal Dish Solar Concentrator Investigations at the ANU – an update*, Proceedings of the international symposium on concentrated solar power and chemical energy technologies, Zurich.

Siebers D.L. and Kraabel J.S. (1984), *Estimating Convective Energy Losses from Solar Central Receivers*, Sandia National Laboratories Report, SAND 84-8717.

Spalart P.R. (2000), *Strategies for Turbulent Modeling and Simulations*, Int. Journal of Heat and Fluid Flow 21, 252-263.

Stine W.B. and McDonald C.G. (1989), *Cavity Receiver Heat Loss Measurements,* presented at ISES World Congress, Kobe, Japan.

Taumoefolau T. (2002), *An Experimental Study of Natural Convection Heat Loss from A Solar Concentrator Cavity Receiver at Varying Orientation*, In Proceedings of ANZSES Annual Conference, Newcastle, Australia.